Semi-Inclusive Deep Inelastic Scattering on a Transversely Polarized He-3 Target Using the BigBite and Super BigBite Spectrometers in Hall A: PAC49 update to E12-09-018

G. Cates (UVa), E. Cisbani (INFN), A. J. R. Puckett (UConn), B. Quinn (CMU),
B. Wojtsekhowski (JLab), E12-09-018 collaboration, and the SBS collaboration

I. INTRODUCTION

We propose precision measurements of single-spin asymmetries (SSAs) in the electroproduction of charged and neutral pions and charged kaons in semi-inclusive deep inelastic scattering (SIDIS) on a transversely polarized, high-luminosity ^{3}He target, using the existing BigBite and Super Bigbite spectrometers at JLab. The proposed measurements, *which will provide statistics roughly 100 times that of any previous study of SSAs in SIDIS for $x \geq 0.1$*, were approved for 64 beam-days in Hall A with an "A-" scientific rating by PAC38 in 2011, as experiment E12-09-018 [1]. In this update document for PAC49, we briefly summarize the developments in the field of SIDIS SSAs and the progress in the preparation of E12-09-018 since PAC38.

In its final report on E12-09-018, PAC38 wrote:

"The PAC endorses the physics goals of the experiment and recognizes that the data is expected be collected on a timescale that would be substantially earlier than the SOLID polarized 3He SIDIS experiment. The data collected will also be at somewhat higher Q2 and higher x than the SOLID experiment; it, therefore, represents a complementary measurement."

Indeed, the situation regarding the timeline of E12-09-018 relative to SOLID and other planned SIDIS measurements with transverse target polarization at JLab has not changed appreciably since PAC38. E12-09-018 can realistically be scheduled as soon as 2023. While the PAC38 report noted the complementarity of kinematic coverages between E12-09-018 and SOLID, we feel that an even stronger statement is justified: in fact, E12-09-018 and SOLID have close to zero overlap in (Q^2, x, y) phase space. At any given beam energy and x value, E12-09-018 will access a higher Q^2 range that is *not even in principle accessible to SOLID*, due to the fact that the SOLID polar angle acceptance only reaches about 25 degrees [2, 3], whereas the BigBite polar angle coverage in E12-09-018 is approximately 25-37 degrees. In SoLID's future study involving kaons, a three-fold improvement of currently achieved time resolution (0.1 ns) will be required [2], whereas E12-09-018 has a clearly identified, proven solution for kaon identification. Note that for $x > 0.5$, SBS SIDIS has comparable statistics and higher Q^2 than SoLID. The final report of the Department of Energy's 2014 review of the SBS project specifically endorsed the scientific importance of E12-09-018, noting:

"The panel reaffirms the scientific importance of the proposed SIDIS measurement enabled by future enhancements to the SBS."

Since PAC38, the SBS program has progressed to a state of readiness for beam, with the installation in Hall A of the first "run group" of experiments [4, 5] on neutron form factors already well underway as of this writing. Moreover, the SBS GEN experiment [6], that will use an upgraded polarized Helium-3 target with performance characteristics similar to those required by E12-09-018, underwent JLab's Experiment Readiness Review (ERR) process in 2020, in anticipation of scheduling as soon as 2022. With the exception of the HERMES RICH detector, all detectors required by E12-09-018 will be commissioned during the GMN run in the fall of 2021, under background rates at least a factor of 10 higher than expected in E12-09-018. The RICH detector components were already extensively tested at the University of Connecticut, and the RICH is currently at Jefferson Lab undergoing preparation for integration into the SBS.

Because the SBS SIDIS experiment will draw so heavily on the hardware that will be used in the first SBS run group, the SBS SIDIS experiment will be ready to run during calendar 2023. E12-09-018 could thus have results on transverse-polarization-related TMD physics well before any other experimental programs that are being planned. Furthermore, regardless of the time scale, the combination of kinematic range and statistical power of the SBS SIDIS experiment is unique among all approved experiments. Given the level of readiness of this experiment, the keen interest in TMDs and nuclear femtography, and the large amount of activity planning for the EIC, we believe that this experiment will produce important insights in a timely manner.
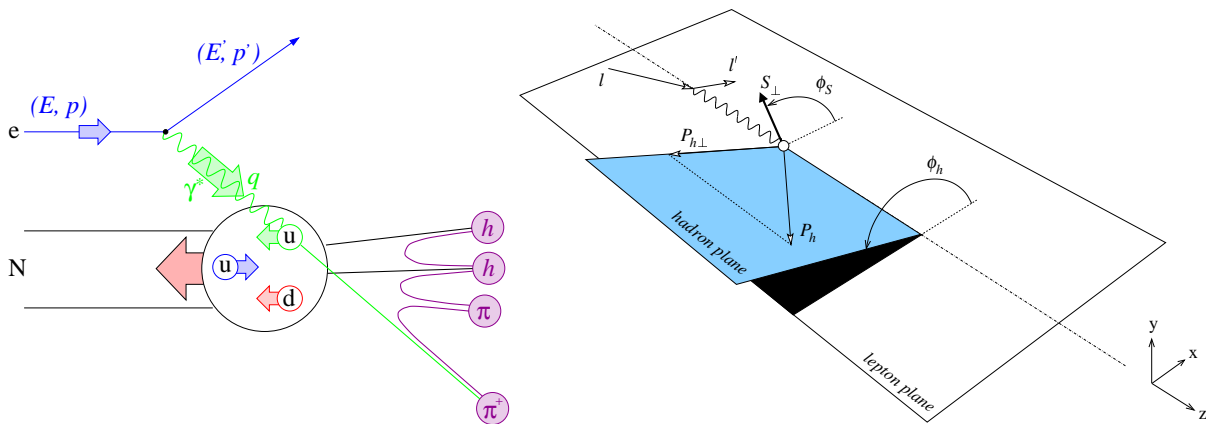
FIG. 1. Left: Conceptual illustration of the SIDIS process. Right: Standard azimuthal angle definitions for SIDIS (figure $P_{h\perp} \equiv \mathbf{p}_T$ in the text).

II. PHYSICS MOTIVATION

The semi-inclusive deep inelastic scattering (SIDIS) process $N(e, e'h)X$, in which a hadron is observed at transverse momentum $\mathbf{p}_T$ (relative to the momentum transfer direction) carrying a large fraction z of the energy absorbed by the struck quark in a deep inelastic lepton-nucleon collision, has emerged in the last several decades as a powerful method for imaging the three-dimensional, spin-dependent quark structure of the nucleon in momentum space. Figure 1 conceptually illustrates the quark-parton-model interpretation of the SIDIS process. The electron undergoes a hard scattering with a quasifree quark in the target nucleon, which then "fragments" into color-neutral hadrons as it recoils from the hard collision.

The energy, azimuthal angle, and transverse momentum distributions of identified hadrons in SIDIS processes carry information about the struck quark's initial transverse momentum $k_\perp$, flavor, and polarization. In fact, in the DIS regime, the cross section "factorizes" as the convolution of a perturbatively calculable hard scattering cross section $d\sigma_{eq\rightarrow eq}$ with a universal transverse momentum dependent (TMD) parton distribution function $f_q(x, k_\perp, Q^2)$, and a universal TMD fragmentation function $D_q^h(z, p_\perp, Q^2)$ (whose $p_\perp$ integrated counterparts $D_q^h(z, Q^2)$ are measured in e^+/e^- annihilation reactions [7–10]). The transverse momenta $\mathbf{k}_\perp$ of the initial quark and $\mathbf{p}_\perp$ of the observed hadron relative to the recoiling quark are unobservable, but are convoluted in the SIDIS observables. To first order in $\mathbf{k}_\perp/Q$, the transverse momentum of the observed hadron is given by [11] $\mathbf{p}_T \approx z\mathbf{k}_\perp + \mathbf{p}_\perp$. Studies of the SIDIS process with polarized beams and targets provide access to spin-orbit correlations that either vanish or are strongly suppressed when integrated over transverse momentum, as in the inclusive DIS process.

Transverse polarization phenomena in SIDIS have attracted ever increasing interest since D. Sivers [12] first proposed a left-right asymmetry in the transverse momentum distribution of unpolarized quarks in a polarized nucleon as a mechanism to explain the large transverse single spin asymmetries observed in inclusive hadron production in $p^\uparrow p \rightarrow h + X$ collisions [13–16]. In the current qualitative interpretation, the single-spin asymmetry in SIDIS on a transversely polarized target arises from two dominant effects: the *Collins* and *Sivers* effects that result from the correlation between the transverse polarization of the target nucleon and, respectively, the transverse polarization and transverse momentum of the struck quark, the latter being connected to quark orbital angular momentum, widely thought to be an important contribution to the proton spin decomposition [17–19]. In the leading-twist approximation, the single-spin asymmetry A_{UT} in SIDIS with an unpolarized lepton beam on a transversely polarized nucleon can be expressed as (see Fig. 1 for the standard angle definitions):

$$A_{UT} \equiv \frac{d\sigma_\uparrow - d\sigma_\downarrow}{d\sigma_\uparrow + d\sigma_\downarrow} = A_{UT}^{Collins}(x, y, Q^2, z, p_T)\sin(\phi_h + \phi_S) + A_{UT}^{Sivers}(x, Q^2, z, p_T)\sin(\phi_h - \phi_S)$$
$$+ A_{UT}^{Pretz}(x, y, Q^2, z, p_T)\sin(3\phi_h - \phi_S) \tag{1}$$

where $d\sigma_{\uparrow(\downarrow)}$ is the cross section with given nucleon transverse polarization, Q^2 is the four-momentum transfer squared, $x = Q^2/(2M\nu)$ is the quark momentum fraction, $y = \nu/E$ is the fractional energy loss by the scattered electron, and $z = E_h/\nu$ is the hadron energy fraction. The third term in Eq. (1), the so-called "pretzelosity" or "Mulders-Tangerman" function, is an allowed leading-twist modulation of A_{UT} that will also be measured by E12-09-018, but which is generally expected to be smaller in magnitude than the Collins or Sivers effects [20–22].

The HERMES and COMPASS experiments pioneered the study of the SIDIS process on transversely polarized targets. In 2009, the HERMES collaboration published the first observation of a non-zero Sivers effect [23] on a proton target for both pion and kaon production, and soon thereafter reported the observation of non-zero Collins effects [24]. The COMPASS collaboration published results on the Collins and Sivers effects for a deuteron target at around the same time [25]. The deuteron results were largely consistent with zero, suggesting a significant cancellation between proton and neutron asymmetries, implying that large asymmetries could be expected on a neutron target, motivating exploratory measurements on a polarized ^{3}He target in JLab's Hall A [26]. The COMPASS collaboration later published results for the proton [27–29], independently confirming the existence of both effects first observed by the HERMES collaboration. Given these discoveries, the study of TMDs and novel transverse spin phenomena in SIDIS and other "hard" processes has emerged as a major worldwide goal of nuclear physics [30], and is also one of the major scientific motivations for the planned US-based Electron-Ion Collider (EIC), which recently received CD-0 and site selection from the US DOE. To go beyond initial exploration and discovery to precision mapping and detailed interpretation of TMD phenomena requires high-statistics data on transversely polarized proton and neutron targets with wide coverage in x and Q^2.

III.   PROGRESS IN TRANSVERSE SPIN PHYSICS SINCE PAC38

In the last 10 years further theoretical studies on the impact of nuclear initial and final states of the ^{3}He on TMD extraction have been carried on beyond the unpolarized SIDIS; their understanding are essential in high-statistics experiments. The Final State Interaction (FSI) in polarized SIDIS has been treated within the generalized eikonal approximation framework; the results [31] are very encouraging: while the transverse spectral function can be quite different in the PWIA approximation respect to more realistic FSI, the extracted TMDs are much less affected by the FSI due to the fact that the effective polarization in the transverse spectral function are combined with the dilution factors; this also supports an affordable flavor decomposition of the TMDs, and then better constraining the d-quark contribution, once new neutron data will be available.

In fact, flavor decomposition is the main goal of the latest COMPASS proposal on transversely polarized ^{6}LiD which is scheduled to run in 2021 [32]. This experiment will produce new data on the deuteron with statistical uncertainties reduced by a factor of 2-5 with respect to the latest extracted COMPASS Transversity data [33]. The new data, combined with the existing proton data and the future JLab neutron data, can be used to extract the u- and d-quark distributions with similar accuracy. It is worth mentioning that the COMPASS phase space ($0.003 \lesssim x \lesssim 0.3$) is complementary to the current proposal.

In the recent years worldwide efforts have been ongoing to perform global fits of the available data on TMDs from lepton-nucleon and Drell-Yan scattering [34, 35]; one relevant question, coming out from these analyses, is the range of applicability and consistencies of the different kinematic regimes [36] and related approximations that are considered for data extraction. From the experimental point of view all recent new transversely polarized TMD data relate to the proton; HERMES revisited its original analysis on the transversely polarized proton data [21], extending the Sivers and Collins asymmetries to larger z; CLAS12 has taken unpolarized deuteron data in 2019 and 2020 which are now under analysis. New polarized data on neutron/deuteron, in barely- or un-explored phase space regions and with precision comparable to the proton data are still highly valuable and beneficial for the global fit analysis and flavor-decomposition, and therefore to ultimately providing an improved picture of the nucleon's 3D structure.

IV.   E12-09-018 EXPERIMENT CONCEPT

While it might seem that a spectrometer with very large angular coverage is the only way to obtain good statistics when studying single-spin asymmetries in SIDIS, the fact is that one can do extremely well by judiciously placing spectrometers with moderately large acceptance. Such an approach also provides flexibility in choosing the kinematics that will be covered. The concept of the E12-09-018 experiment is based on the fact that there is strong kinematic focusing of hadrons with high z along the direction of the momentum transfer $\vec{q}$. The acceptance of the spectrometer must still be moderately large, however, to obtain coverage of a sufficient range of p_T. This is precisely the philosophy of E12-09-018, in which we use two large open-geometry dipoles, providing around 40-50 msr of solid angle each. Of course, single-spin asymmetries require studying the azimuthal-angular distributions of the hadrons. This is the azimuthal angle around the momentum-transfer vector $\vec{q}$, however, not the azimuthal angle around the beam direction. By centering a spectrometer such as SBS on $\vec{q}$, one can obtain excellent azimuthal coverage where it is most important. Finally, the azimuthal angle of interest must be referenced to the direction of the target polarization, and it is important to have the flexibility to orient the polarization within the plane that is perpendicular to $\vec{q}$, something that is straightforward with a polarized ^{3}He target that operates at a modest field of tens of Gauss.
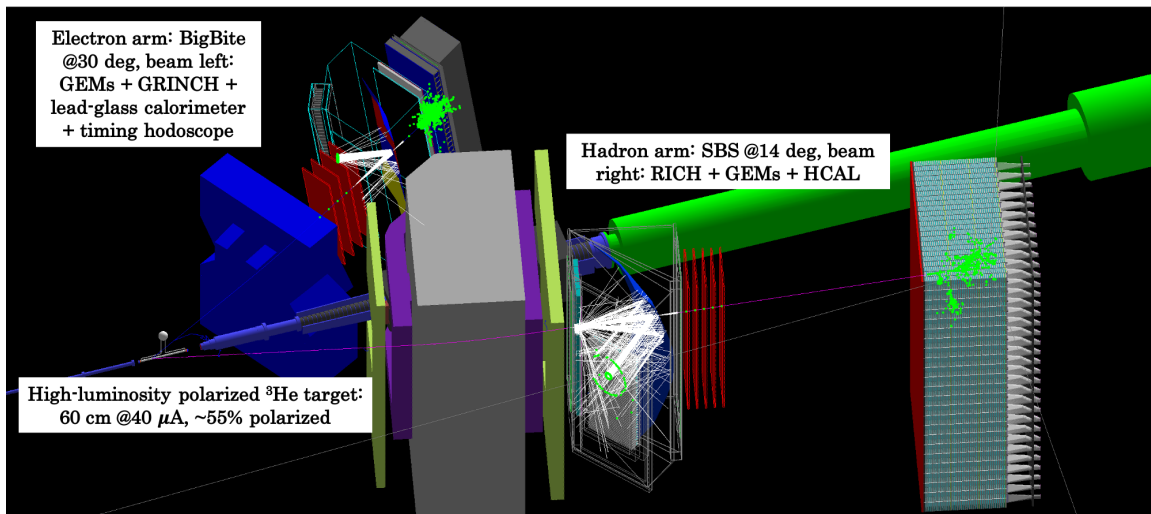
FIG. 2. Screenshot of one ^{3}He$(e, e'\pi^+)X$ event, tracked through the E12-09-018 layout in *g4sbs*, the GEANT4-based Monte Carlo simulation package for the SBS experiments. For clarity, details of the He-3 target infrastructure other than the target cell itself (e.g., magnetic shielding box, Helmholtz coils, etc) are not shown.

Another advantage of the dipole spectrometers is the sweeping of low energy backgrounds out of the acceptance by their magnets, allowing comfortable operation of the detectors with the polarized He-3 target at a total electron-nucleon luminosity of 3×10^{37} Hz/cm^2. Thus, the combination of BigBite, SBS and a polarized ^{3}He target make it possible to obtain a dramatic increase in statistics of roughly two orders of magnitude or more compared to all previous studies of single-spin asymmetries in SIDIS. Furthermore, E12-09-018 probes a kinematic regime, including high-x and relatively large Q^2, that has not previously been studied.

E12-09-018 will detect coincidences between scattered electrons and either a pion or kaon produced in deep inelastic collisions with polarized ^{3}He. The electron will be detected by an upgraded version of the BigBite spectrometer which has been used previously for multiple experiments in Hall A. The pion or kaon will be detected by the Super Bigbite Spectrometer (SBS), which will undergo commissioning during the initial SBS program measuring elastic nucleon form factors at high momentum transfer. BigBite will be set at a central angle of 30°, and comprises a ~ 1 T·m dipole magnet with vertical bend, a tracking system with five layers of GEMs, a gas Cherenkov detector for offline pion rejection, a scintillator hodoscope for precise timing, and a two-layer lead-glass calorimeter that will be used for both triggering and additional pion rejection. The SBS will be placed at a central angle of 14 degrees, and is based on a large dipole magnet with vertical bend and a slot cut in its yoke to facilitate running at a small angle despite its considerable size. The SBS magnet will be operated at an integral of approximately 1.7 T·m, the same field at which SBS will operate during the first of the SBS experiments (to measure G_M^n). The SBS detector package includes six layers of GEMs, a ring imaging Cherenkov detector (the RICH, previously used in HERMES), and a large hadron calorimeter (HCAL) that accommodates the full acceptance of the two spectrometers. HCAL will provide a trigger, modest energy resolution and will also assist in spatially constraining events (for both the RICH and the GEMs), a useful role at the high rates at which we will be running. HCAL will also provide detection for neutral pions.

The basic layout of the experimental setup can be seen in Figure 2, which shows a screenshot of a single SIDIS ^{3}He$(e, e'\pi^+)X$ event from the SBS GEANT4-based Monte Carlo simulation package *g4sbs*. The close proximity of the spectrometers to the target is clearly evident, which is critical for maximizing our angular acceptance. While not explicitly visible in the figure, it is easy to imagine why a cut in the SBS magnet's yoke was needed to make it possible to set the spectrometer to small angles. Extensive calculations of the magnetic fields were performed using TOSCA during the design process of SBS itself, and to understand the overall magnetic field environment of the full experimental setup, including the regions of the target and the detectors. The primary triggers of the experiment will come from BigBite's lead-glass calorimeter and HCAL, respectively corresponding to electrons with energies $E'_e \geq 1$ GeV, and charged or neutral hadrons with momentum $p_h \geq 2.0$ GeV. The HCAL is placed as far away from the target as possible without reducing the acceptance. This provides for time-of-flight based charged hadron identification at lower momenta, and also improves the neutral pion reconstruction by increasing the separation between the two π^0 decay photons at the surface of HCAL. The moderately large solid-angle acceptance and the essentially unlimited momentum acceptance of both BigBite and SBS allow the proposed experiment to cover most of the relevant kinematic phase space for fixed-target SIDIS with an 11 or 8.8 GeV beam in a single spectrometer setting.

V. PROJECTED RESULTS

In preparation for the proposal that was approved by PAC38 [1], we carried out an exhaustive simulated analysis using a fast Monte Carlo simulation with parametrized acceptances and detector resolutions for SBS and BigBite. We generated high-statistics pseudo-data sets with close to the full proposal statistics, with the kinematics of generated events distributed according to the acceptance-convoluted SIDIS cross sections using a rejection sampling method, with "built-in" target SSAs according to the global fits of Ref. [37] for the transversity and Collins functions and Ref. [38] for the Sivers functions. We then analyzed these simulated data sets using a maximum-likelihood method, to obtain accurate statistical uncertainty projections for our proposed data [39], and to demonstrate the validity of our asymmetry extraction method. Since PAC38, we have implemented detailed models of the SBS and BigBite detectors, magnets and magnetic fields, targets, and beamlines in GEANT4 (see Figure 2). For this update to PAC49, we have performed new, but lower-statistics simulations using *g4sbs* with the same cross section model used for the original proposal as a cross check of the SIDIS event rates and kinematic coverage estimates from PAC38. We summarize our new results in table I, which shows the projected total statistics of ^{3}He$(e, e'h)X$ events for $h = \pi^+, \pi^-, K^+, K^-$, and π^0, applying "standard" SIDIS kinematic cuts as described in the Tab. I caption, and requiring tracks in the BigBite and SBS GEMs, above-threshold signals in the BigBite and SBS calorimeters, and adequate signal for pion rejection (hadron PID) in the BigBite (SBS) Cherenkov counter. For π^0 events, both photons were required to hit HCAL, with a minimum separation of 30 cm. For this PAC49 update, as in the PAC38 proposal, we assume 40 μA beam current on a 60-cm target, for a total electron-nucleon luminosity of approximately 1.2×10^{37} cm^{-2} s^{-1} (^{3}He only). We note that the statistics shown in Tab. I agree with the rates from the original proposal to within about 10% for all beam energies and hadrons considered. The phase space coverages do not differ substantially from those presented in the original proposal, and are shown in Figure 3.

E_e (GeV)	Days	^{3}He$(e, e'\pi^+)X$ Events/10^6	^{3}He$(e, e'\pi^-)X$ Events/10^6	^{3}He$(e, e'K^+)X$ Events/10^6	^{3}He$(e, e'K^-)X$ Events/10^6	^{3}He$(e, e'\pi^0)X$ Events/10^6
11	40	104	69	14	2.4	17
8.8	20	101	57	14	2.1	15

TABLE I. Total projected ^{3}He$(e, e'h)X$ statistics in the PAC38-approved E12-09-018 beam time at 11 and 8.8 GeV by hadron, after applying all relevant calorimeter, track, and Cherenkov cuts in both spectrometers. Kinematic cuts applied are $Q^2 > 1$ GeV^2, $W^2 > 4$ GeV^2, $M_X^2 > 2.3$ GeV^2, $p_T \geq 0.05$ GeV, $E_e' \geq 1$ GeV and $p_h \geq 2$ GeV. In addition, adequate signals in the BigBite and SBS detectors were required as described in the text. Full statistical projections for Collins and Sivers asymmetries $\vec{n}(e, e'h)X$, as evaluated for the original PAC38 proposal, are tabulated in Ref. [39].

Extracting the Sivers and Collins moments requires good coverage of the azimuthal angle around the momentum transfer vector $\vec{q}$. As described in the previous section, the kinematical focusing of high-z hadrons, together with the placement of SBS, greatly helps in achieving that goal. Another important factor in achieving the needed coverage in azimuthal angle is the ability to orient the polarization of the target in various directions spanning the plane that is perpendicular to $\vec{q}$. In our original proposal, we envisioned eight such orientations, corresponding to being parallel or antiparallel to four separate directions. In order to minimize changes to the G_E^n polarized ^{3}He target, however, we are instead planning to use four target orientations, corresponding to what we can refer to as horizontal or vertical orientations, together with spin flips. Restricting ourselves to four target orientations greatly simplifies the polarized target, and most importantly, has only negligible effect on our azimuthal coverage, which is summarized in Figure 4. Restricting ourselves to four target orientations also means that we can benefit from our experience during the Transversity run group [26].

Ultimately, the value of E12-09-018 is the truly dramatic increase in statistics that will be obtained in a timely manner. The interest in TMDs in the nuclear physics community is huge, and large numbers of papers are being written on the basis of a data set that has not changed appreciably in a decade. E12-09-018 will provide statistical figure-of-merit for the neutron that is typically *two orders of magnitude* higher than existing proton data [23, 29], and 2-3 orders of magnitude higher than existing deuteron [25] or neutron [26] data. Kinematically, the coverage will be excellent at high Bjorken-x, and will extend low enough in x to overlap regions that have already been studied. As just one example of the statistical power of E12-09-018, we show in Figure 5-left a comparison of our projected data with published proton and deuteron data from HERMES and COMPASS. Except at the highest x values, our error bars are too small to be viewed in a meaningful way in Figure 5-left, so in Figure 5-right we show a figure of merit (FOM) of our projected statistics as a function of x_{Bj}, along with the corresponding FOM of the published HERMES and COMPASS proton data, COMPASS deuteron data, and E06-010 neutron data. It is important to note that the figure-of-merit shown in Fig. 5-right is obtained by taking the reciprocal square of the published asymmetry uncertainty, and is *not* corrected for the differences in x bin width between the published data sets, which use variable x bin widths,
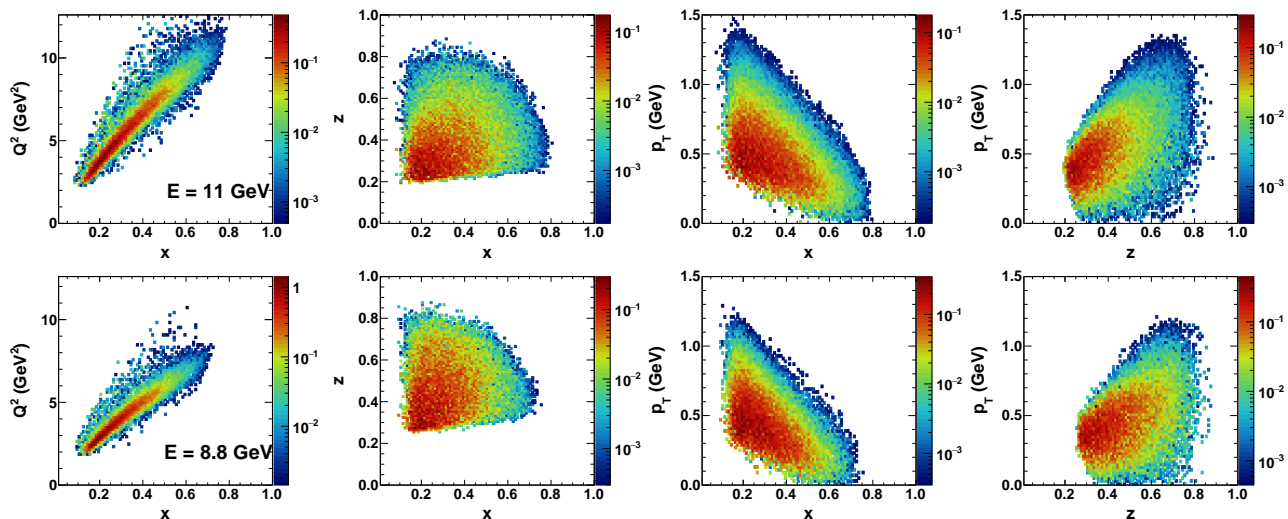
FIG. 3. SIDIS kinematic coverage of E12-09-018 for 11 GeV (top row) and 8.8 GeV (bottom row) beam energy, obtained using *g4sbs* (compare to Fig. 5.1 of the PAC38 proposal [1]). From left to right: Q^2 vs. x, z vs. x, p_T vs. x, and p_T vs. z. Cuts applied are $Q^2 \geq 1$ GeV^2, $W^2 \geq 4$ GeV^2, $M_X^2 \geq 2.3$ GeV^2, $E'_e \geq 1$ GeV, and $p_h \geq 2$ GeV, and good signals in all relevant detectors. No minimum p_T cut is applied for these plots, but such a cut is included in the projected statistics shown in Table I. The color scale is proportional to the event yield, but its absolute normalization is arbitrary.
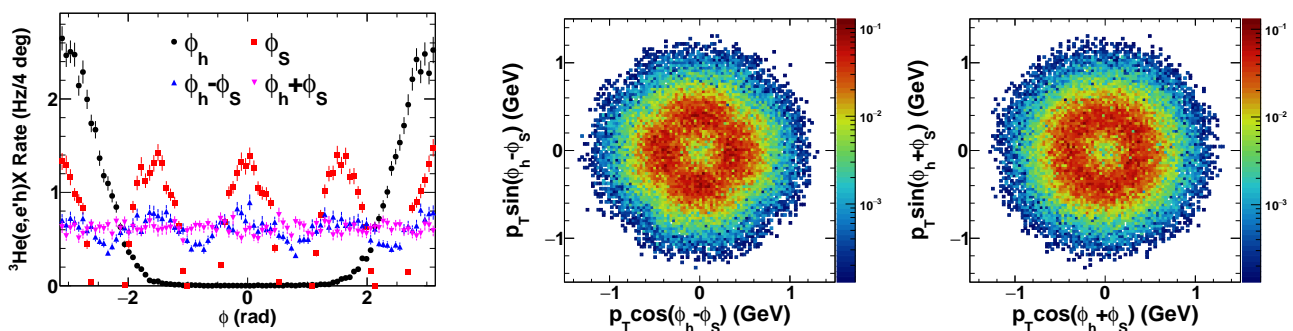

FIG. 4. Rate-weighted SIDIS azimuthal angle coverage in E12-09-018 with four target spin directions (instead of the eight envisioned by the original proposal). The simulated coverages shown are for ^{3}He$(e, e'h)X$ events at 11 GeV, summed over all charged hadrons h ($h = \pi^+, \pi^-, K^+, K^-$). The ϕ_h coverages are independent of the charged hadron species and are essentially identical (in fact slightly better) at 8.8 GeV. The ϕ_h coverage for ^{3}He$(e, e'\pi^0)X$ events is only slightly worse than for charged hadrons due to the reduced acceptance for π^0's. The 1D distributions on the left are integrated over all kinematic variables other than ϕ_h, ϕ_S. The 2D color plots on the right show the $(p_T, \phi_h \pm \phi_S)$ coverage in polar coordinates. In these plots, the color scale is proportional to the event rate.

and the projected E12-09-018 data, which are shown using a constant bin width $\Delta x = 0.1$ (for $0.1 \leq x \leq 0.7$). In particular, the FOM comparison shown in Fig. 5-right significantly *understates* the improvement that E12-09-018 will provide for $x \geq 0.1$, as the highest x bins used by the HERMES and COMPASS analyses are significantly wider than the fixed bin width of $\Delta x = 0.1$ assumed in the E12-09-018 projections presented to PAC38 [39].

VI. PROGRESS IN PREPARATION OF THE EXPERIMENT

This experiment was first proposed in 2009 after the DOE approved funding for the SBS and BigBite spectrometers for the high-momentum-transfer nucleon-form-factor program. Our proposal drew on the successful experience in Hall A with the first polarized ^{3}He single-spin asymmetry measurement, the availability of the RICH detector used during the HERMES experiment, and the demonstration at UVa of a novel convection-based polarized ^{3}He target capable of handling higher luminosities. In the intervening time, an enormous amount of progress has been achieved. SBS and a significantly upgraded version of the BigBite spectrometer are now being installed in Hall A for the first SBS run
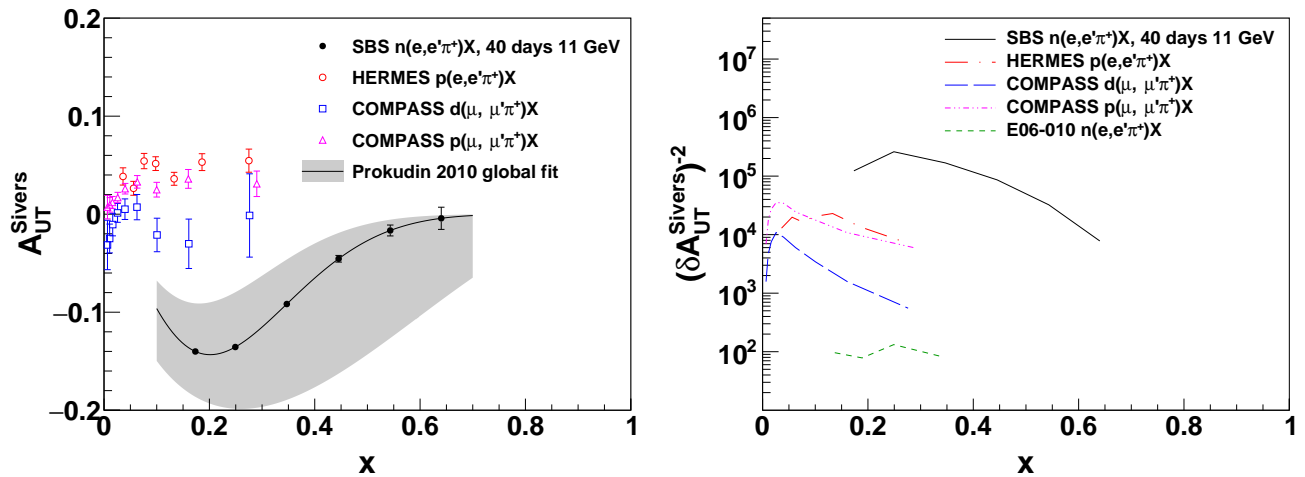
FIG. 5. Left: projected Sivers asymmetry precision for $\vec{n}(e, e'\pi^+)X$ from E12-09-018 (11 GeV data only), with the same uniform x binning presented in the PAC38 proposal [1, 39], compared to published proton data from HERMES [23] and proton and deuteron data from COMPASS [25, 29], as well as the prediction of a 2010 global fit by A. Prokudin with central value (black solid curve) and uncertainty band (gray shaded region) evaluated for the kinematics, acceptances, and cuts of E12-09-018. Right: Statistical figure-of-merit, defined as the reciprocal square of the asymmetry uncertainty, for the example data shown in the left plot, *uncorrected* for differences in x bin width among the various data sets.

group. The HERMES RICH has been refurbished and is at JLab. Also, a high-luminosity convection-style polarized ^{3}He target has been used successfully in Hall C, and an even higher luminosity polarized ^{3}He target has been largely constructed and will be installed for the SBS G_E^n experiment at the conclusion of the first SBS run group. In short, the SBS SIDIS experiment is rapidly approaching a state of readiness to run in the immediate future.

A. Transversely polarized He-3 target

The target for the SIDIS experiment, E12-09-018, will make maximal use of the hardware that has been developed for the SBS polarized ^{3}He experiment (E12-09-016), which underwent a readiness review in October of 2020. The G_E^n target, as we will refer to it herein, represents a substantial upgrade from the target that was recently used in Hall C for measurements of both the spin asymmetry A_1^n and the twist-three matrix element d_2^n. In particular, the G_E^n target is designed to run at $60\,\mu$A rather than $30\,\mu$A, and presents the electron beam with twice the target thickness (of ^{3}He) as was the case during the A_1^n/d_2^n runs, resulting in up to a factor of three increase in figure of merit. Furthermore, the G_E^n target will also be fully enclosed in a more-or-less cube-shaped soft-iron magnetic shield which insures that, even near the BigBite and SBS magnets, magnetic field inhomogeneities are held well within acceptable values, an important improvement over the target used in Hall C.

While the G_E^n target will represent a major upgrade from the recent Hall C target, we should mention that the Hall C target achieved in excess of a factor of two improvement in figure-of-merit over all polarized ^{3}He targets that had been used previously in electron scattering. All of the polarized ^{3}He target cells that have been used at JLab have comprised two chambers, the target chamber, through which the electron beam passes, and the pumping chamber, in which the ^{3}He is polarized. The Hall C target was the first to use our so-called "convection design", which allows full control over the speed with which ^{3}He is moved between the target and pumping chambers respectively [40]. This allowed us to take full advantage of the speed with which the ^{3}He was polarized, and allowed us to run at $30\,\mu$A rather than $12-15\,\mu$A, the maximum beam currents used previously, while maintaining a polarization in beam of over 50%.

The main difference in requirements between the SIDIS and G_E^n polarized ^{3}He targets is the orientation of the nuclear polarization. In our original SIDIS proposal, we described using eight separate target directions. Upon further analysis, however, we have found that limiting ourselves to four distinct target directions has negligible effects on our results, and greatly simplifies the needed target modifications. These four directions include two in the horizontal plane (parallel to one another but pointing in opposite directions), and two in the vertical direction (again, parallel but pointing in opposite directions). All of these target orientations are roughly perpendicular to the direction of the momentum transfer. The single-spin asymmetries we will be studying will involve spin flips in the horizontal and vertical orientations respectively.

The modifications needed to the G_E^n target are well defined, and not extensive. When the polarization is in a

horizontal direction, the only requirement is that the target ladder will need to be rotated (about its vertical axis) to an orientation that is different from those that will be used during G_E^n. The oven that houses the G_E^n target's pumping chamber, along with associated optics, is already designed to operate from arbitrary directions (in the horizontal plane), so the only significant change involves re-positioning the optics on top of the target enclosure in order to point the laser beams in the required directions. Re-positioning the optics is reasonably straight forward because of the development of what we call "one-inch optics modules", compact free standing modules that each deliver 50 Watts or more to the target, and that were first used in the aforementioned Hall C target.

For the vertical polarization orientation, four notable but straightforward changes are needed. First, we must rotate the magnetic-field coils so that they can provide a vertical field. Second, we will attach the aforementioned one-inch optics modules directly to the target ladder so that they can point downwards at the target cell with no bounces off of mirrors. Third, we will use a target cell with two pumping chambers as is illustrated in the right-hand panel of Figure 6. The two-pumping chamber design was actually explored extensively during the development stage of the G_E^n target. We moved to the current G_E^n design, with a simpler single pumping chamber, by adding to our design the ability to illuminate our target cells from two directions. When orienting the polarization vertically, however, the simplest approach is to return to the two-pumping-chamber design and illuminate each pumping chamber from a single direction from above. The fourth notable change is that we will need a new forced-hot-air oven to accommodate the two pumping chambers. We note for completeness that rotating the magnetic-field coils to provide a vertical field is likely to take roughly one week, where our estimate is based on recent experience rotating the magnetic-field coils of the Hall C polarized ^{3}He target.
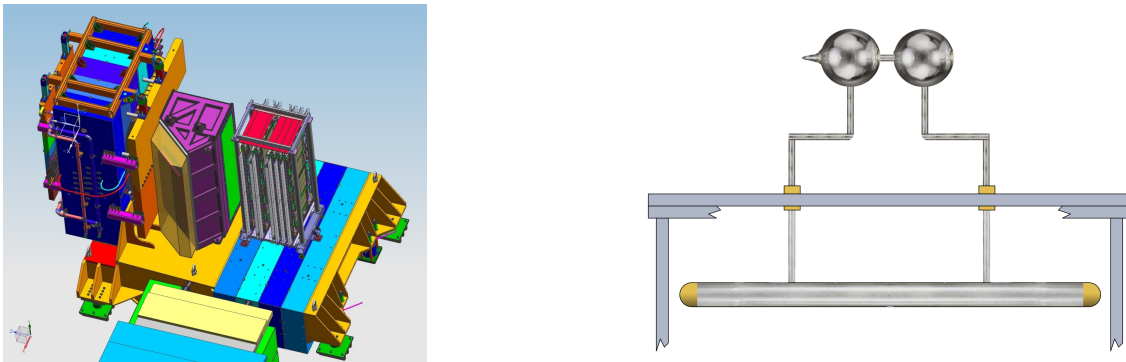

FIG. 6. Left: SBS detector package for E12-09-018 in the 3D CAD model of Hall A. Right: Model of the SIDIS target cell.

We close our discussion of the polarized ^{3}He target by mentioning that, overall, much of what we are planning is reproducing capability that was already demonstrated during the "Transversity" run group, which included E06-010, the earlier JLab experiment that studied single-spin asymmetries in SIDIS. For E06-010, however, an additional large pair of coils was used to produce the vertical field. In contrast, for E12-09-018, we will limit the polarization directions to a single vertical plane (more-or-less perpendicular to the beam direction), which will allow us to use two sets of coils rather than three. By only using two sets of coils (as will be the case for G_E^n) the target will be more compact, allowing us to use most of the G_E^n target hardware, including, for example the soft-iron magnetic shield and most of the components contained therein.

B. BigBite spectrometer

The SBS equipment currently being installed in Hall A includes an upgraded version of the BigBite spectrometer, which will be positioned at 30° from the beamline, with the magnet yoke front face at 155 cm from the target center. The BigBite upgrades include a five-plane GEM tracker, which provides greatly improved high-rate capability. Also included is the "GRINCH" detector which will provide electron identification by using heavy gas and imaging the Cherenkov ring to a small cluster of tubes on an array of 500 PMTs. The pre-shower (9.5 cm thick lead-glass read by 52 PMTs) and total-absorbtion shower counter (read by 189 PMTs) have been carefully checked and refurbished, as needed. A finely-spaced timing hodoscope (read out by 180 PMTs) is positioned between the pre-shower and shower counters.

These detectors were tested individually, and as a package, on site before being moved into Hall A and installed on BigBite (see Fig. 7-c). Cabling of the detectors in the Hall will begin in July. The solid angle spanned by the detectors will be 45 msr. BigBite and the detector package will be used extensively this year and next so they will be very well understood by the time of running of SIDIS.
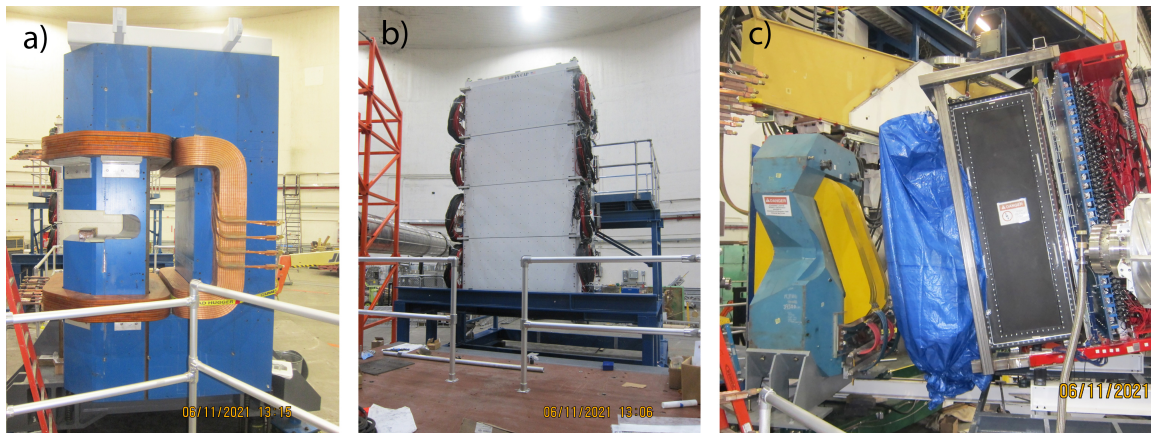
FIG. 7. Shown are some of the major components of the SBS program being installed in Hall A during June of 2021, including a) the SBS magnet, b) HCAL, and c)the BigBite spectrometer.

C. Super Bigbite spectrometer (SBS)

The hadron arm will be the SBS which, for this experiment, will consist of a large vertical-bend dipole magnet (48D48); a Ring Imaging Cherenkov (RICH), described below; a high-resolution tracker composed of six GEM planes, which provide high-rate capability; and a 288-module Hadron Calorimeter (HCal).

The magnet system is being assembled in Hall A, (see Fig. 7-a). It will be commissioned this fall and experience with its use and positioning will be gained this year and next. The magnet yoke will be positioned 280 cm from the target at $14°$ from the beamline. The large aperture will cover $\pm 3.6°$ horizontally and $\pm 12°$ vertically. The GEMs for SBS have been built; testing is continuing, using cosmic rays, on site. Operational experience will be gained with these detectors this year during the G_M^n run group. HCal was tested and calibrated on site with pulsers and cosmic rays. It was moved to Hall A and assembled this spring (see Fig. 7-b) and cabling will begin in July. Experience with positioning, data-taking and data-analysis of HCal will be gained this year and next.

D. RICH detector

The RICH detector for SBS consists of one of the two HERMES RICH modules [41] which was moved to JLab for the purpose of E12-09-018, once it was realized that its geometry and performance characteristics were very well matched to those of the SBS magnet and detectors. In fact, the SBS hadron setup closely resembles one half of the HERMES spectrometer, oriented vertically. The photon detector for the RICH consists of a matrix of 1,934 3/4-inch PMTs, which have been thoroughly re-tested and characterized in the last few years. The original PCOS4 based front-end and back-end electronics have been replaced by more recent NINO-chip based front-end cards that will be read out by already procured VETROC back-end modules that also provide high-resolution timing information, that will allow for a reduction of the effective occupancy of the RICH PMTs to 0.1% or less in offline analysis, which poses no significant problems for the PID analysis. The Monte Carlo simulation of the RICH in SBS, validated by the HERMES data, was used to evaluate the PID performance at the full luminosity of E12-09-018. The refurbished RICH with upgraded electronics will guarantee PID performance similar to or even better than the original HERMES RICH. Figure 8 shows the reconstructed Cherenkov emission angles and a single event display from the HERMES RICH [41].

E. Collaboration

E12-09-018 is an SBS collaboration experiment. The collaboration includes more than 50 active members from 18 institutions including institutions from the U.S., Canada, the UK, Armenia, and several INFN institutes in Italy. The SBS-experiments currently include E12-07-109(GEp), E12-09-016(GEn), E12-09-019(GMn), E12-09-018(SIDIS), C12-15-006 (TDIS), E12-17-004 (GEn-recoil), E12-20-008 (Pion-KLL), E12-20-010 (nTPE), and run group addition C12-15-006A (TDIS-Kaon). We note that the SIDIS experiment (E12-09-018), like all the SBS experiments, is well integrated into the structure of the SBS program, in part through the SBS Coordinating Committee, which includes

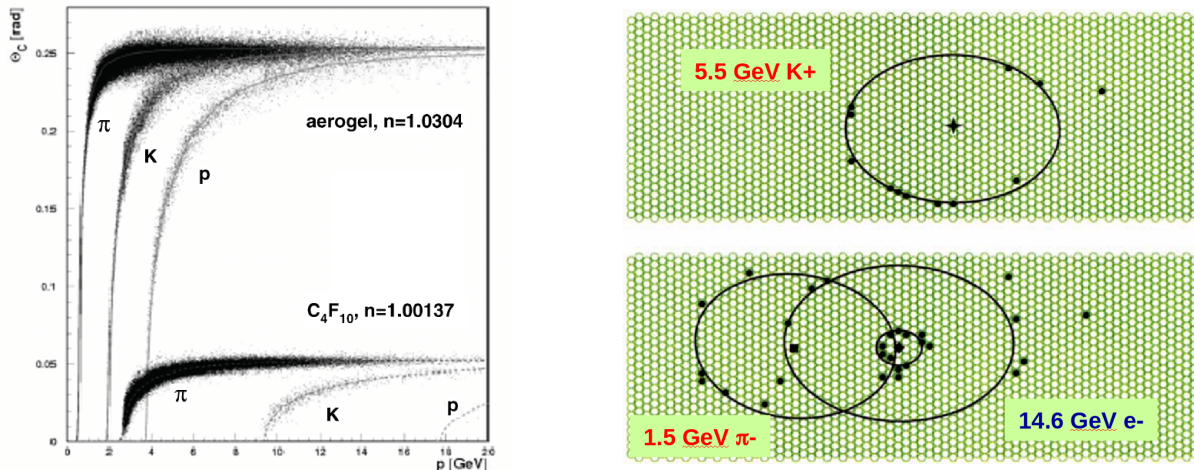representatives of all approved SBS experiments.

FIG. 8. Left: cumulative data of the HERMES RICH angular distribution versus hadron momentum. Right: A single event display with three different particle types and momenta [41].

VII.   SUMMARY AND BEAMTIME REQUEST

We have presented an update to E12-09-018 (approved by PAC38) to measure single-spin asymmetries (SSAs) in semi-inclusive deep inelastic scattering (SIDIS). The experiment will provide a dramatic improvement (~ 100 in statistics) in our understanding of polarization-dependent Transverse Momentum Distributions (TMDs), a subject in which there is tremendous interest within the nuclear physics community. Indeed, the study of TMDs is a central motivation for building the EIC. Despite the importance of TMDs, there has been a dearth of new data in this field for roughly a decade, and there are no approved experiments that will study transverse-polarization-related TMDs for many years to come. Also, regardless of timescale, the combination of kinematic range and statistical accuracy of E12-09-018 is unique.

In contrast to when we presented E12-09-018 to PAC38, almost all the components needed have already been constructed, and many of them are in the process of being installed in Hall A for the first SBS run group. The only equipment needed for E12-09-018 that will not be fully tested as part of the initial SBS program will be the refurbished HERMES RICH and a set of straightforward modifications to the G_E^n polarized ^{3}He target that will facilitate the needed polarization directions. In short, the E12-09-018 is already in an advanced stage of readiness.

Our beam-time request is the same as in our original proposal and is summarized below:

	Time (day)
Production run at $E = 11$ GeV	40
Production run at $E = 8.8$ GeV	20
Calibration Runs	2
Target maintenance and configuration changes	2
Total	64

The table above is unchanged from that approved by PAC38. In keeping with PAC49 guidelines, we would also like to request the scheduling of one week without beam to change the target configuration from horizontal polarization to vertical polarization. As explained in Section VI A, this will enable considerable simplification of the SIDIS target design, allowing us to minimize modifications of the G_E^n target for use in SIDIS.

------

[1] G. Cates, E. Cisbani, G. Franklin, A. Puckett, B. Wojtsekhowski, *et al.*, Target Single-Spin Asymmetries in Semi-Inclusive Pion and Kaon Electroproduction on a Transversely Polarized ^{3}He Target using Super BigBite and BigBite in Hall A (2011), http://hallaweb.jlab.org/collab/PAC/PAC38/SBS-SIDIS.pdf.

[2] The SoLID Collaboration (2019), `https://hallaweb.jlab.org/12GeV/SoLID/files/solid-precdr-Nov2019.pdf`.

[3] H. Gao, X. Qian, J. P. Chen, X. Jiang, *et al.*, Target Single Spin Asymmetry in Semi-Inclusive Deep-Inelastic $(e, e'\pi^{\pm})$ Reaction on a Transversely Polarized ^{3}He Target at 8.8 and 11 GeV (2010), `http://www.jlab.org/exp_prog/proposals/10/PR12-10-006.pdf`.

[4] R. Gilman, B. Quinn, B. Wojtsekhowski, *et al.*, Precision Measurement of the Neutron Magnetic Form Factor up to $Q^2 = 18.0$ (GeV/c)^2 by the Ratio Method (2007), `http://www.jlab.org/exp_prog/proposals/07/PR12-07-109.pdf`.

[5] J. R. M. Annand, V. Bellini, M. Kohl, N. Piskunov, B. Sawatzky, and B. Wojtsekhowski, Measurement of the ratio G_E^n/G_M^n by the double-polarized $^2H(\vec{e}, e'\vec{n})$ reaction (2017), `https://www.jlab.org/exp_prog/proposals/17/PR12-17-004.pdf`.

[6] G. Cates, S. Riordan, B. Wojtsekhowski, *et al.*, Measurement of the Neutron Electromagnetic Form Factor Ratio G_E^n/G_M^n at High Q^2 (2009), `http://hallaweb.jlab.org/collab/PAC/PAC34/PR-09-016-gen.pdf`.

[7] S. Kretzer, Fragmentation functions from flavor-inclusive and flavor-tagged e^+e^- annihilations, Phys. Rev. D **62**, 054001 (2000).

[8] S. Albino, B. Kniehl, and G. Kramer, Fragmentation functions for light charged hadrons with complete quark flavour separation, Nuclear Physics B **725**, 181 (2005).

[9] M. Hirai, S. Kumano, T.-H. Nagai, and K. Sudoh, Determination of fragmentation functions and their uncertainties, Phys. Rev. D **75**, 094009 (2007).

[10] D. de Florian, R. Sassot, and M. Stratmann, Global analysis of fragmentation functions for pions and kaons and their uncertainties, Phys. Rev. **D75**, 114010 (2007), arXiv:hep-ph/0703242 [HEP-PH].

[11] A. Bacchetta, F. Delcarro, C. Pisano, M. Radici, and A. Signori, Extraction of partonic transverse momentum distributions from semi-inclusive deep-inelastic scattering, Drell-Yan and Z-boson production, JHEP **06**, 081, [Erratum: JHEP06,051(2019)], arXiv:1703.10157 [hep-ph].

[12] D. W. Sivers, Single Spin Production Asymmetries from the Hard Scattering of Point-Like Constituents, Phys.Rev. **D41**, 83 (1990).

[13] R. D. Klem, J. E. Bowers, H. W. Courant, H. Kagan, M. L. Marshak, E. A. Peterson, K. Ruddick, W. H. Dragoset, and J. B. Roberts, Measurement of asymmetries of inclusive pion production in proton-proton interactions at 6 and 11.8 gev/c, Phys. Rev. Lett. **36**, 929 (1976).

[14] W. H. Dragoset, J. B. Roberts, J. E. Bowers, H. W. Courant, H. Kagan, M. L. Marshak, E. A. Peterson, K. Ruddick, and R. D. Klem, Asymmetries in inclusive proton-nucleon scattering at 11.75 gev/ c, Phys. Rev. D **18**, 3939 (1978).

[15] S. Saroff *et al.*, Single Spin Asymmetry in Inclusive Reactions Polarized P, P Goes to π^+, π^-, and P at High P(t) at 13.3-GeV/c and 18.5-GeV/c, Phys. Rev. Lett. **64**, 995 (1990).

[16] D. Adams *et al.*, Analyzing power in inclusive π^+ and π^- production at high xf with a 200 gev polarized proton beam, Physics Letters B **264**, 462 (1991).

[17] A. Deur, S. J. Brodsky, and G. F. De Téramond, The Spin Structure of the Nucleon, Rept. Prog. Phys. **82**, 10.1088/1361-6633/ab0b8f (2019), arXiv:1807.05250 [hep-ph].

[18] C. A. Aidala, S. D. Bass, D. Hasch, and G. K. Mallot, The Spin Structure of the Nucleon, Rev. Mod. Phys. **85**, 655 (2013), arXiv:1209.2803 [hep-ph].

[19] M. Boglione and A. Prokudin, Phenomenology of transverse spin: past, present and future, Eur. Phys. J. **A52**, 154 (2016), arXiv:1511.06924 [hep-ph].

[20] Y. Zhang *et al.* (Jefferson Lab Hall A), Measurement of pretzelosity asymmetry of charged pion production in Semi-Inclusive Deep Inelastic Scattering on a polarized ^{3}He target, Phys. Rev. **C90**, 055209 (2014), arXiv:1312.3047 [nucl-ex].

[21] A. Airapetian *et al.* (HERMES), Azimuthal single- and double-spin asymmetries in semi-inclusive deep-inelastic lepton scattering by transversely polarized protons, JHEP **12**, 010, arXiv:2007.07755 [hep-ex].

[22] S. Boffi, A. V. Efremov, B. Pasquini, and P. Schweitzer, Azimuthal spin asymmetries in light-cone constituent quark models, Phys. Rev. D **79**, 094012 (2009), arXiv:0903.1271 [hep-ph].

[23] A. Airapetian *et al.* (HERMES Collaboration), Observation of the naive-t-odd sivers effect in deep-inelastic scattering, Phys. Rev. Lett. **103**, 152002 (2009).

[24] A. Airapetian *et al.*, Effects of transversity in deep-inelastic scattering by polarized protons, Physics Letters B **693**, 11 (2010).

[25] M. Alekseev *et al.*, Collins and sivers asymmetries for pions and kaons in muon–deuteron {DIS}, Physics Letters B **673**, 127 (2009).

[26] X. Qian *et al.* (Jefferson Lab Hall A), Single Spin Asymmetries in Charged Pion Production from Semi-Inclusive Deep Inelastic Scattering on a Transversely Polarized ^{3}He Target, Phys. Rev. Lett. **107**, 072003 (2011), arXiv:1106.0363 [nucl-ex].

[27] M. Alekseev *et al.*, Measurement of the collins and sivers asymmetries on transversely polarised protons, Physics Letters B **692**, 240 (2010).

[28] C. Adolph *et al.*, {II} – experimental investigation of transverse spin asymmetries in μp {SIDIS} processes: Sivers asymmetries, Physics Letters B **717**, 383 (2012).

[29] C. Adolph *et al.* (COMPASS), Collins and Sivers asymmetries in muonproduction of pions and kaons off transversely polarised protons, Phys. Lett. B **744**, 250 (2015), arXiv:1408.4405 [hep-ex].

[30] M. Anselmino, A. Mukherjee, and A. Vossen, Transverse spin effects in hard semi-inclusive collisions, Progress in Particle and Nuclear Physics **114**, 103806 (2020).

[31] A. Del Dotto, L. P. Kaptari, E. Pace, G. Salmè, and S. Scopetta, Final state interactions and the extraction of neutron single spin asymmetries from semi-inclusive deep-inelastic scattering by a transversely polarized ^{3}He target, Phys. Rev. **C96**, 065203 (2017), arXiv:1704.06182 [nucl-th].

[32] O. Denisov, J. Friedric, C. Collaboration, and PNPI, d-Quark Transversity and Proton Radius. Addendum to the

COMPASS-II Proposal (2018), `https://wwwcompass.cern.ch/compass/proposal/2021/compass_prop_2017_v4_0.pdf`.

[33] A. Martin, B. F., and B. V., Extracting the transversity distributions from single-hadron and dihadron production, PRD **1**, 014034 (2015).

[34] M. G. Echevarria, Z.-B. Kang, and J. Terry, Global analysis of the sivers functions at nlo+nnll in qcd, Journal of High Energy Physics **2021**, 10.1007/jhep01(2021)126 (2021).

[35] A. Bacchetta, F. Delcarro, C. Pisano, and M. Radici, The three-dimensional distribution of quarks in momentum space (2020), arXiv:2004.14278 [hep-ph].

[36] M. Boglione, A. Dotson, L. Gamberg, S. Gordon, J. Gonzalez-Hernandez, A. Prokudin, T. Rogers, and N. Sato, Mapping the kinematical regimes of semi-inclusive deep inelastic scattering, Journal of High Energy Physics **2019**, 10.1007/jhep10(2019)122 (2019).

[37] M. Anselmino, M. Boglione, U. D'Alesio, A. Kotzinian, F. Murgia, A. Prokudin, and S. Melis, Update on transversity and collins functions from {SIDIS} and data, Nuclear Physics B - Proceedings Supplements **191**, 98 (2009).

[38] M. Anselmino, M. Boglione, U. D'Alesio, A. Kotzinian, S. Melis, *et al.*, Sivers Effect for Pion and Kaon Production in Semi-Inclusive Deep Inelastic Scattering, Eur.Phys.J. **A39**, 89 (2009), arXiv:0805.2677 [hep-ph].

[39] G. Cates, E. Cisbani, G. Franklin, A. Puckett, B. Wojtsekhowski, *et al.* (2011), `https://userweb.jlab.org/~puckett/PR1209018/KineTables/`.

[40] P. A. M. Dolph, J. Singh, T. Averett, A. Kelleher, K. E. Mooney, V. Nelyubin, W. A. Tobias, B. Wojtsekhowski, and G. D. Cates, Gas dynamics in high-luminosity polarized he targets using diffusion and convection, Phys. Rev. C **84**, 065201 (2011).

[41] N. Akopov *et al.*, The {HERMES} dual-radiator ring imaging cherenkov detector, Nuclear Instruments and Methods in Physics Research Section A: Accelerators, Spectrometers, Detectors and Associated Equipment **479**, 511 (2002).